



HAL
open science

Catalytic coatings on stainless steel prepared by sol–gel route

Dimitri Truyen, Matthieu Courty, Pierre Alphonse, Florence Ansart

► **To cite this version:**

Dimitri Truyen, Matthieu Courty, Pierre Alphonse, Florence Ansart. Catalytic coatings on stainless steel prepared by sol–gel route. *Thin Solid Films*, 2006, 495 (1-2), pp.257-261. 10.1016/j.tsf.2005.08.200 . hal-03598173

HAL Id: hal-03598173

<https://hal.science/hal-03598173>

Submitted on 4 Mar 2022

HAL is a multi-disciplinary open access archive for the deposit and dissemination of scientific research documents, whether they are published or not. The documents may come from teaching and research institutions in France or abroad, or from public or private research centers.

L'archive ouverte pluridisciplinaire **HAL**, est destinée au dépôt et à la diffusion de documents scientifiques de niveau recherche, publiés ou non, émanant des établissements d'enseignement et de recherche français ou étrangers, des laboratoires publics ou privés.

Catalytic coatings on stainless steel prepared by sol–gel route

Dimitri Truyen, Matthieu Courty, Pierre Alphonse and Florence Ansart

CIRIMAT, UMR-CNRS 5085, Université Paul Sabatier, 118 route de Narbonne, 31062
Toulouse Cedex 4, France

Abstract

Stainless steel (flat and microstructured) substrates have been coated with sol–gel catalysts made up of metal nanoparticles (Rh, Ni, Pt) dispersed on alumina and alumina–ceria supports. The aluminum monohydroxyde (boehmite) sols were synthesized by hot hydrolysis/peptization of an aluminum alkoxide (Yoldas method). It is shown that the rheological properties of the sol, especially the thixotropy, play a key role on the homogeneity and the quality of the film deposited on the metal substrate. The catalyst layers have a very good adhesion, a thickness which can be easily controlled (in the range 0.1 to 10 μm), a large specific surface area and a good mechanical and thermal stability.

Keywords: Sol–gel; Alumina; Thixotropy; Catalytic film

1. Introduction
 2. Experimental
 - 2.1. Synthesis of sols
 - 2.2. Rheology of the sols
 - 2.3. Coating of the metallic substrates
 - 2.4. Characterization of catalysts
 3. Results and discussion
 - 3.1. Xerogels
 - 3.2. Coatings
 - 3.3. Catalytic activity of the coatings
 4. Conclusion
- Acknowledgements
References

1. Introduction

Metal catalysts, supported on porous refractory oxides, are generally deposited on ceramic substrates. These substrates are appropriate for high temperature applications but they have some disadvantages. They are brittle, slow down thermal transfers, do not allow an optimal use of catalyst and their cost is rather high. Their replacement by a metal substrate would allow these drawbacks to be avoided. Moreover, effective catalyst deposition techniques on a metal substrate enable the elaboration of microstructured reactors, made up by stacking metal plates grooved with several parallel channels covered with catalyst. Such reactors have many advantages [1] like a large improvement of the thermal and mass transfers, very short response times, an optimization of the catalyst amount and a better safety. Moreover, stainless steel microstructured reactors are more resistant to mechanical stresses (expansions, compressions, vibrations).

In this paper, a process suitable for coating microstructured steel reactor with catalyst layers is reported. In order to enhance the exchange surface area between gaseous reactants and catalyst, porous oxides like SiO_2 , ZrO_2 , TiO_2 or Al_2O_3 are generally used as carriers. In this study, the catalyst support was alumina, chosen because of its high surface area and thermal stability. Several active metals as rhodium, nickel and platinum have been dispersed on the alumina carrier. The coating synthesis procedure was sol-gel route because it is a simple, low temperature process, well suited for film deposition, allowing particle size control, and a large range of composition. Sol-gel also allows the synthesis of thin catalyst layers which leads to an optimal use of expensive precious metals.

2. Experimental

2.1. Synthesis of sols

The synthesis of the alumina sols, precursors of the catalyst layers, was based on the method originally proposed by Yoldas [2], [3], [4] and [5]. The first step of the process was the hydrolysis of aluminum alkoxide (in this work we have used aluminum tri-sec-butoxide, $\text{Al}(\text{OC}_4\text{H}_9)_3$ —Acros Organic) at 85 °C in a large excess of water ($\text{H}_2\text{O} / \text{Al} = 100$). This gave an aluminum hydroxide slurry that was subsequently peptized to a clear sol by addition of nitric acid ($\text{HNO}_3 / \text{Al} = 0.07$).

For nickel catalysts, $\text{Ni}(\text{CH}_3\text{COO})_2 \cdot 4 \text{H}_2\text{O}$ —Prolabo Analytical or $\text{Ni}(\text{HCOO})_2 \cdot 2 \text{H}_2\text{O}$ —Alfa Aesar, have been used as precursors. The required amount of the precursor, dissolved in the minimum amount of water, was added after peptization. For precious metal catalysts, the rhodium ($\text{RhCl}_3 \cdot x \text{H}_2\text{O}$ —Acros Organic) or the platinum ($\text{H}_2\text{PtCl}_6 \cdot 6 \text{H}_2\text{O}$ —Prolabo Analytical) precursor was dissolved in the water used for the hydrolysis. For ceria–alumina carrier, the ceria precursor ($\text{Ce}(\text{NO}_3)_3 \cdot 6 \text{H}_2\text{O}$ —Acros Organic or $\text{Ce}(\text{CH}_3\text{COO})_3 \cdot 1.5 \text{H}_2\text{O}$ —Sigma Aldrich) dissolved in the minimum amount of water, was added after peptization. Yoldas [4] suggested that the peptization can be done by an acid solution containing the water soluble salt. But it has been observed that, under these conditions, the peptization becomes very slow and several days are needed to obtain a clear sol. Therefore we have chosen to add the solution of the ceria precursor after the complete peptization.

After peptization, the sols were concentrated by heating at 85 °C, until they became thixotropic. Microstructural characterizations have been done on thin films of gel coated on PTFE substrates. After drying at room temperature, the film could be easily separated from the substrate. These xerogels were reduced to powders by simple grinding.

2.2. Rheology of the sols

A rotational viscometer (Rheoanalyzer, Contraves, Gieres, France) equipped with coaxial cylinders was used to study the sol viscosity. A MS-DIN 1301 unit was used for the diluted sols (Newtonian fluid) and a MS-DIN 125 unit for the concentrated sols. The shear stress was recorded (at room temperature) while the rate of shear was first increased up to 1000 s^{-1} in 150 s and then decreased back to zero, also in 150 s.

A thixotropic fluid undergoes a decrease in viscosity with time while it is subjected to shearing. Therefore when the shear rate was increased to a certain value, then decreased back to zero, the “up” and “down” plots of shear stress versus shear rate do not coincide. The area of the “hysteresis loop” have been used as a measure of the thixotropy.

2.3. Coating of the metallic substrates

The first step was the surface treatment of the stainless steel in order to ensure an optimal adhesion between the layer and the substrate. In this operation, the plates were immersed in an alkaline cleaner (Turco™ 4181) at 75 °C for 30 min. Then they were rinsed with water in an ultrasound bath. Finally they were dried and heated in air at 500 °C for 2 h.

On flat steel substrates, the coating was performed by the dip-coating technique whereas it was done by tape casting on microstructured substrates, in such a way that the sol remained only inside the microchannels. After coating, the plates were dried overnight at room temperature. The final step was a calcination in air, at a temperature in the range 500 to 800 °C, for 2 h.

The maximum thickness obtained from concentrated sols was about 3 μm . To prepare thicker layers, sols have been loaded with powders prepared by firing gels of the same composition. These powders were incorporated into the sols under stirring until a homogeneous mixture was obtained. This method allows to prepare thick layers of good quality because the shrinkage is strongly reduced during the drying step.

2.4. Characterization of catalysts

The crystal structure was investigated by powder X-ray diffraction (PXRD). Data were collected on a Seifert 3003TT θ - θ diffractometer in the Bragg-Brentano geometry, using filtered Cu K α radiation and a graphite secondary-beam monochromator. Diffraction intensities were measured by scanning from 5° to 90° (2θ) with a step size of 0.02° (2θ).

Scanning electron microscopy (SEM) analyses were done on a JEOL JSM-6700 (equipped with a field emission gun). Transmission electron microscopy (TEM) analyses were carried out on a JEOL 2010. For these analyses, a small amount of powder was put in ethanol and dispersed in an ultrasound bath during 1 min. Then the carbon-coated grid was dipped in the suspension and allowed to dry at room temperature.

The nitrogen adsorption-desorption isotherms and the krypton adsorption isotherms were determined at 77 K by volumetric method with a Micromeritics ASAP 2010 device.

The thickness of the films was determined either by using a white light interferometer (Zygo New Niew 100 system) or by SEM from a cross-section image.

3. Results and discussion

3.1. Xerogels

Xerogels prepared without addition of metal precursor only contain nanosized crystals of boehmite. On heating, the boehmite structure was maintained up to 400 °C, then progressive

transformation in transition alumina (η -alumina) occurred. The η -alumina structure was stable up to 800 °C [6]. Whatever the heating temperature, the alumina catalysts are essentially mesoporous with no macroporosity and little microporosity [7]. The average pore diameter increased from 3 nm at 400 °C to 8 nm at 800 °C. The porous volume, about 0.3 cm³/g, did not change much with temperature. The specific surface area reached a maximum at 450 °C (close to 500 m²/g). Above this temperature it decreased almost linearly (150 m²/g at 800 °C).

Xerogels containing 7 or 10 wt.% of nickel have been synthesized from two precursors, nickel acetate and nickel formate. Very little differences were found between nickel–alumina and pure alumina on XRD patterns and on nitrogen adsorption–desorption isotherms (Table 1). Reduction under H₂ gave Ni/alumina catalysts. When the reduction was performed at 500 °C, the metallic crystallites were very well distributed in alumina and they were very small, in the range 1–3 nm. After reduction at higher temperature sintering began but, in contrast with classical Ni/alumina catalysts, growth remained rather limited (Fig. 1). The crystallites remained very small even above 800 °C (in the range 4–8 nm for 800 °C). It can be noticed that the size of nickel particles was similar to the size of pores. This can be explained if the metallic particles are trapped in the pores of alumina which inhibits the diffusion of metal atoms and reduces the sintering. Catalysts prepared from nickel formate precursor were found slightly less thermally stable.

Table 1.

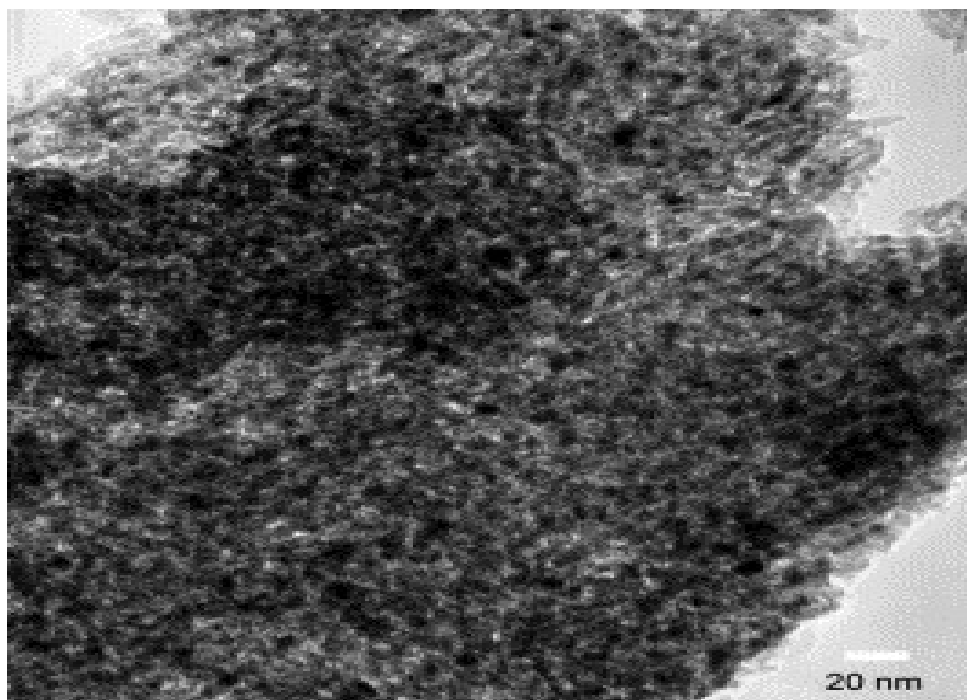
Effect of the addition of platinum and ceria on the porosity of alumina

	S_{BET} (m ² g ⁻¹)	Pore volume (cm ³ g ⁻¹)	Average pore diameter, d_h (nm)
Alumina—500 °C	330	0.33	4.0
Alumina—700 °C	240	0.30	5.0
Alumina—800 °C	150	0.27	7.2
3.9% ceria (nitrate)—alumina—500 °C	308	0.29	3.8
10% ceria (nitrate)—alumina—500 °C	277	0.22	3.2
20% ceria (nitrate)—alumina—500 °C	250	0.22	3.5
10% ceria (nitrate)—alumina—800	170	0.27	6.3

	S_{BET} ($\text{m}^2 \text{g}^{-1}$)	Pore volume ($\text{cm}^3 \text{g}^{-1}$)	Average pore diameter, d_h (nm)
$^{\circ}\text{C}$			
10% ceria (acetate)–alumina—500 $^{\circ}\text{C}$	330	0.31	3.7
10% ceria (acetate)–alumina—700 $^{\circ}\text{C}$	220	0.28	5.1
10% ceria (acetate)–alumina—800 $^{\circ}\text{C}$	165	0.26	6.3
7% Ni (acetate) on alumina—500 $^{\circ}\text{C}$	360	0.34	3.8
7% Ni (acetate) on alumina—700 $^{\circ}\text{C}$	240	0.31	5.2
1% Rh on alumina—700 $^{\circ}\text{C}$	230	0.28	4.9
2% Rh on alumina—800 $^{\circ}\text{C}$	190	0.29	6.1
1% Pt on alumina—500 $^{\circ}\text{C}$	380	0.37	3.9
1% Pt on alumina—700 $^{\circ}\text{C}$	260	0.34	5.2
1% Pt on alumina—800 $^{\circ}\text{C}$	160	0.31	7.8
1% Pt on 10% ceria–alumina—500 $^{\circ}\text{C}$	330	0.30	3.6
1% Pt on 10% ceria–alumina—700 $^{\circ}\text{C}$	220	0.27	4.9

The BET and pore volume are calculated from the nitrogen adsorption isotherms (the mean pore diameter d_h is calculated assuming a cylindrical pore geometry, S_{BET} being taken as the pore surface area, $d_h = 4 V / S$).

Fig. 1. TEM micrograph of a 10% Ni–alumina powder (prepared from nickel acetate) after reduction at 820 °C in H₂ (JEOL 2010 Transmission Electron Microscope).



Xerogels containing 1 and 2 wt.% of rhodium have been prepared using RhCl₃ as precursor. TEM micrographs of Rh/alumina samples heated under air showed no difference with pure alumina. EDS analysis indicated that Rh was uniformly distributed in alumina carrier. It was impossible to detect the presence of Rh in the X-ray diffraction patterns even for the 2%-catalysts.

Sols containing 1 wt.% of platinum have been prepared using H₂PtCl₆ as precursor. Whatever the firing temperature, the presence of Pt in alumina increased the total pore volume and the specific surface area of alumina ([Table 1](#)).

It is well known that the catalytic activity of Pt metal is most often enhanced when ceria is added in the alumina carrier [8], [9] and [10]. Therefore we have also synthesized ceria–alumina gels using two different precursors, cerium acetate and cerium nitrate. Addition of ceria induced a decrease of both the pore volume and the specific surface area. Slightly higher surface areas were obtained when Ce–acetate precursor was used ([Table 1](#)).

Powder X-ray diffraction patterns of platinum/ceria/alumina catalysts (prepared from Ce–nitrate) are reported in Fig. 2. The addition of ceria has delayed the crystallization of alumina, nevertheless the lines of cubic CeO₂ (calculated pattern at the bottom of the graph) are visible. With Ce–acetate precursor, for the same Ce concentration, the diffraction peaks of cerium oxide are less strong. The lines of CeO₂ almost disappeared after a reduction of the catalyst in hydrogen at 500 °C. After this reduction, the main line (111) of metallic platinum are barely visible. As with Rh–alumina catalysts, transmission electron microscopy did not allow the detection of the platinum particles because of the lack of contrast between the carrier and the metal crystallites (Fig. 3).

Fig. 2. Effect of cerium concentration on XRD patterns of Pt/Ce–Al catalysts calcined at 500 °C in air; cerium precursor is nitrate ($\lambda_{Cu} = 0.154184$ nm).

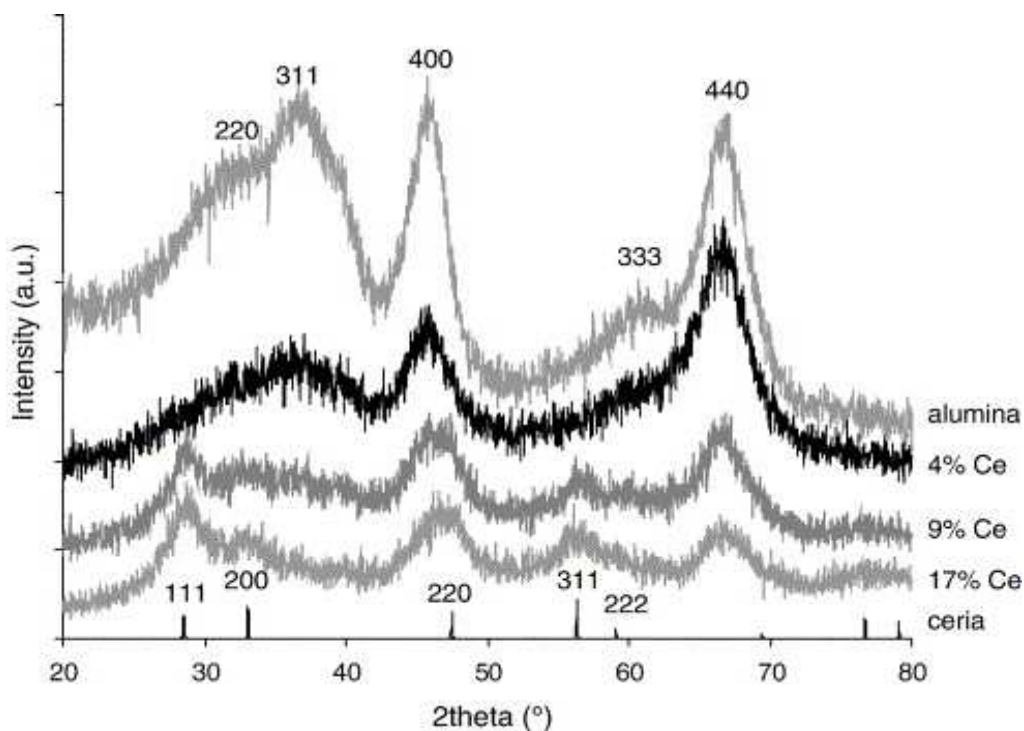
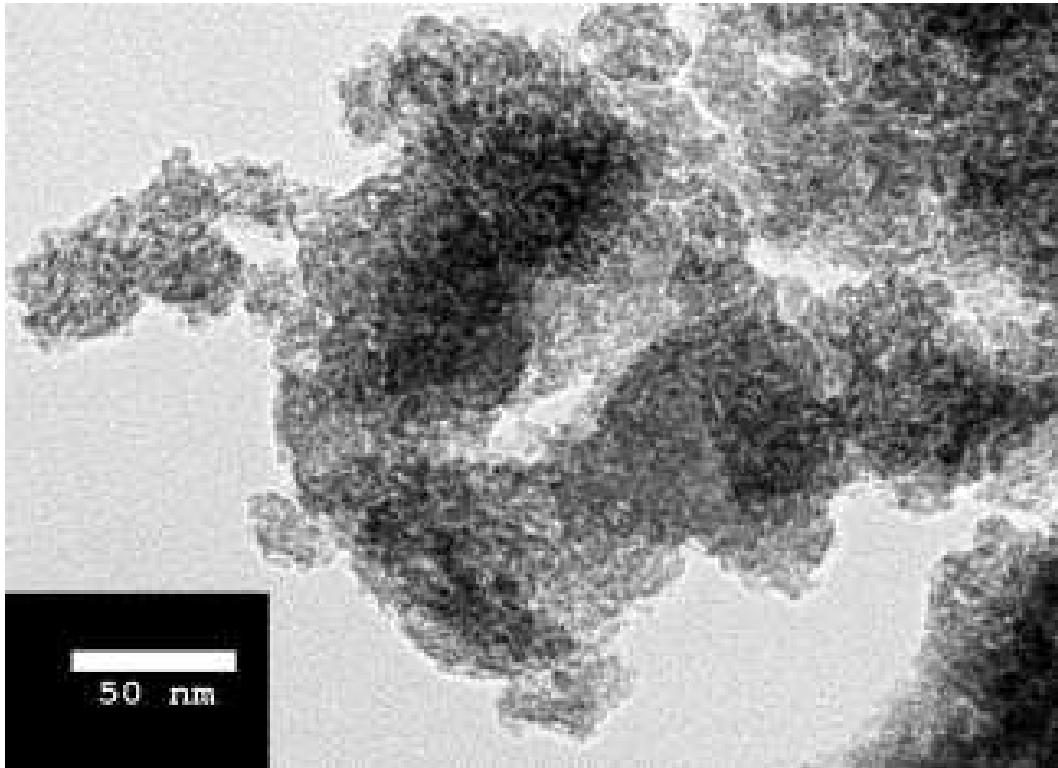


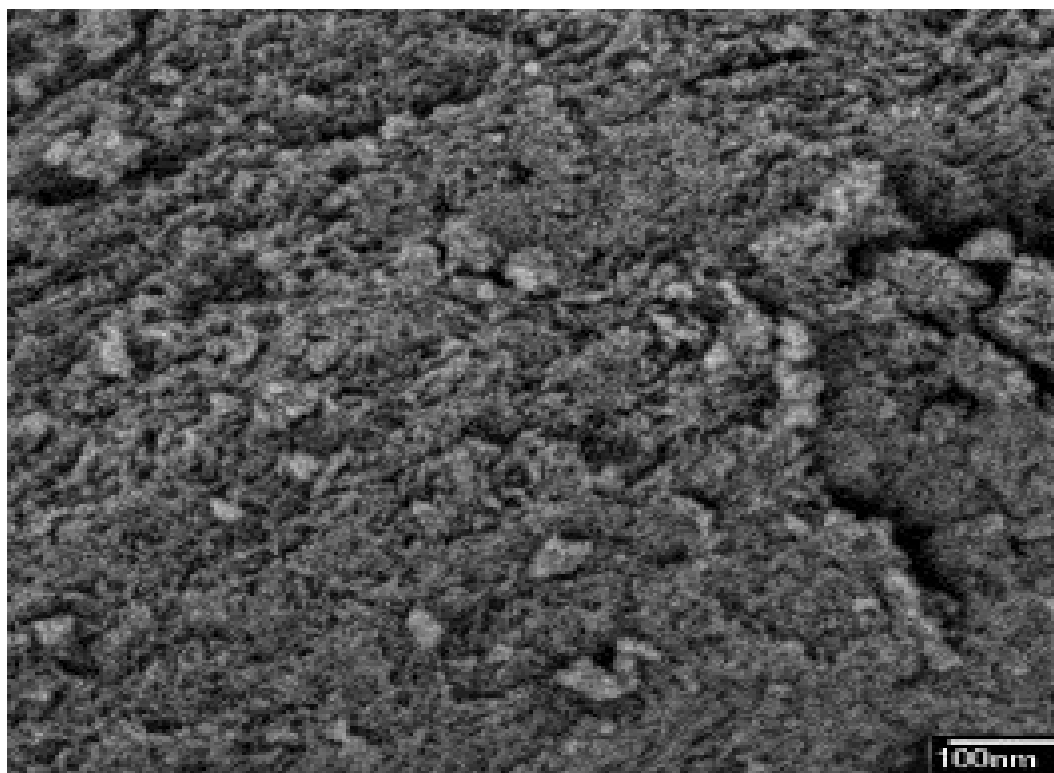
Fig. 3. TEM of 2% Pt on 9% Ce–alumina powder after calcination at 500 °C in air (JEOL 2010 Transmission Electron Microscope).



3.2. Coatings

When the clear colloidal sol of boehmite, directly prepared from Yoldas process, was used to coat metallic substrates, nonhomogeneous films were obtained. Moreover the layer thickness was low (about 100 nm). This is caused by the low viscosity of the sol. However it was rather difficult to increase the viscosity only by concentrating the sol because the viscosity remained stable up to the sol–gel transition where it drastically changed in a very short period of time. It was noticed that, close to the transition zone, before gelation, the sol became thixotropic (see [experimental section](#)). This is linked to the creation of a loose network between the particles leading to the building of a tri-dimensional structure. Both the particle shape and the possibility of hydrogen bonding between the hydroxyl groups at the surface of the particles, play a role in this behavior. It was also observed that the presence of compounds like acetate or formate induces the formation of thixotropic sols without concentrating. It has been found that thixotropic sols allowed the preparation of homogenous coatings on stainless steel. The thickness of the layer depended on the sol concentration as well as on its viscosity. These films were strongly adherent. The very porous texture of these layers is clearly shown by SEM ([Fig. 4](#)).

Fig. 4. SEM of 2% Pt on 9% Ce–alumina film after calcination at 500 °C in air (JEOL JSM-6700 Field Emission Gun Scanning Electron Microscope).



The surface area of the catalysts coated on flat or microstructured platelets has been studied by gas adsorption. Due to the low surface areas involved, krypton has been used as the adsorbate. The surface enhancement factor (SEF), expressed in m^2/m^2 , is defined as the ratio of the real surface area (as measured by gas adsorption) over the geometric surface. The values of the SEF, as calculated from surface area measurements by Kr adsorption on substrates coated with various catalysts, have been reported in [Table 2](#). In order to help the interpretation of the data, in the last column the ratio of the SEF to the coating thickness has also been calculated.

Table 2.

Surface Enhancement Factors (SEF) of coatings

Catalyst	Coating thickness (μm)	SEF (m ² m ⁻²)	SEF/μm (m ² m ⁻² μm ⁻¹)
7% Ni (acetate) on alumina—500 °C	1.5	1340	900
7% Ni (acetate) on alumina—700 °C	1.5	920	600
10% Ni (acetate) on alumina—500 °C	3.5	3230	900
10% Ni (acetate) on alumina—700 °C	3.5	1740	500
1% Rh on alumina—500 °C	3.4	3030	900
1% Rh on alumina—500 °C	2.6	2350	900
1% Pt on 10% Ce (acetate)–alumina—500 °C	1.2	1200	1000
1% Pt on 10% Ce(NO ₃) ₃ –alumina—500 °C	1.1	1000	900
1% Pt on 10% Ce(NO ₃) ₃ –alumina—500 °C+ powder	8.6	7700	900
1% Pt on 10% Ce(NO ₃) ₃ –alumina—500 °C+ powder	12.3	10300	840

SEF is defined as the ratio of the real surface area (measured by Kr adsorption at 77 K) over the geometric surface of the substrate.

For all of the alumina coatings, the SEF was found to be proportional to the thickness of the film, about 900 m²/m² per micron (for coatings calcined at 500 °C). As demonstrated in the case of nickel catalysts, increasing the firing temperature decreased the SEF. On the other hand, the amount of catalyst coated on stainless steel substrates has been evaluated from the weight difference after and before the coating. From these values and the real surface area given by krypton adsorption, the specific surface area of the layer has been calculated. This value, about 300 m²/g for samples heated at 500 °C, is very close to the specific surface area found with unsupported films.

From the results obtained with ceria–alumina catalysts it can be concluded that, i) the surface area was similar for both Ce–nitrate and Ce–acetate precursors, ii) almost the complete catalyst surface area remained accessible to Kr even when the thickness of the layer increased, iii) loading sols with catalyst powder did not decrease the surface area.

3.3. Catalytic activity of the coatings

These catalyst films have been deposited on the walls of microstructured reactors and tested for several gas-phase reactions. The Rh–alumina catalysts were tested for octane autothermal

reforming [11]. Pt/ceria–alumina catalysts were tested for High Temperature Water Gas Shift [12] and Ni–alumina catalysts are currently tested for CO methanation. In all cases, their activities were found better or similar than those of classical catalysts of the same composition.

4. Conclusion

This work demonstrates that a modified process, initially based on the method originally proposed by Yoldas, allows to easily synthesize a wide variety of metal–alumina coatings on stainless steel substrates. The homogeneity and the quality of the film were optimal when the sol was thixotropic. In this case, the layers have a very good adhesion. The thickness can be controlled either by the sol concentration (in the range 0.1 to 3 μm) or by addition of powder of the same composition. These coatings have a large specific surface area and a good thermal stability. When used to coat microstructured reactors, this effective deposition technique has given better or similar catalytic activities than those of conventional catalytic systems.

Acknowledgements

This research was done in the frame of the MINIREF (ENK6-CT-2001-00515) project supported by the E.C.

References

G. Kolb and V. Hessel, *Chem. Eng. J.* 98 (2003), p. 1.

B.E. Yoldas, *J. Mater. Sci.* 10 (1975), p. 1856.

B.E. Yoldas, *Am. Ceram. Soc. Bull.* 54 (1975), p. 286.

B.E. Yoldas, *Am. Ceram. Soc. Bull.* 54 (1975), p. 289.

B.E., Yoldas. US Patent, 3,941,719 (1976).

P. Alphonse and M. Courty, *Thermochim. Acta* 425 (2005), p. 75.

P. Alphonse and M. Courty, *J. Colloid. Interface Sci.* 290 (2005), p. 208.

J.S. Church, N.W. Cant and D.L. Trimm, *Appl. Catal., A Gen.* 101 (1993) (1), p. 105.

A. Vazquez, T. Lopez, R. Gomez, X. Bokhimi, A. Morales and O. Novaro, *J. Solid State Chem.* 128 (1997), p. 161.

A. Piras, A. Trovarelli and G. Dolcetti, *Appl. Catal., B Environ.* 28 (2000), p. L77.

H. Ehrich, U. Kürschner, P. Alphonse, G. Kolb, H. Ehwald and EHEC, *2nd European Hydrogen Energy Conference, Nov 22nd–25th, 2005–Zaragoza* (2005).

G. Germani, P. Alphonse, M. Courty, Y. Schuurman, C. Mirodatos, *Catal. Today* (in press).

Corresponding author. Tel./fax: +33 0561556285.

Original text : Elsevier.com